Icarus 208 (2010) 1–10

Contents lists available at ScienceDirect

Icarus

journal homepage: www.elsevier.com/locate/icarus

Coupled thermal–orbital evolution of the early Moon

Jennifer Meyer *, Linda Elkins-Tanton, Jack Wisdom

Massachusetts Institute of Technology, Cambridge, MA 02139, USA

ARTICLE INFO

Article history:
Received 6 August 2009
Revised 4 January 2010
Accepted 28 January 2010
Available online 4 February 2010

Keywords:
Moon
Earth
Satellites, Dynamics

ABSTRACT

Coupled thermal–orbital histories of early lunar evolution are considered in a simple model. We consider a plagioclase lid, overlying a magma ocean, overlying a solid mantle. Tidal dissipation occurs in the plagioclase lid and heat transport is by conduction and melt migration. We find that large orbital eccentricities can be obtained in this model. We discuss possible consequences of this phase of large eccentricities for the shape of the Moon and geochronology of lunar samples. We find that the orbit can pass through the shape solution of Garrick-Bethell et al. (Garrick-Bethell, I., Wisdom, J., Zuber, M. [2006]. Science 313, 652), but we argue that the shape cannot be maintained against elastic deformation as the orbit continues to evolve.

1. Introduction

Garrick-Bethell et al. (2006) argued that the shape of the Moon could be explained if the Moon froze in its shape while its orbit was eccentric and the rotation state was either synchronous or in the 3:2 commensurate state (as is Mercury). For synchronous rotation the implied orbit is $a = 22.9R_E$, $e = 0.49$, and for the 3:2 spin–orbit state the orbit is $a = 24.8R_E$, $e = 0.17$, where a is the semimajor axis of the lunar orbit and e is the orbital eccentricity. There are two questions to be addressed by this hypothesis: can evolutionary scenarios be generated such that the lunar orbit passes through the shape solutions, and can the shape of the Moon be frozen in at this epoch?

Past studies of the evolution of the lunar orbit have largely ignored the evolution of the eccentricity, and focused instead on the evolution of the orbital inclination (e.g. Goldreich, 1966; Touma and Wisdom, 1994). One exception is Touma and Wisdom (1998), in which the evolution of the lunar orbit through the evection and eviction resonances was studied. Large eccentricities were obtained, but at an earlier epoch (and smaller semimajor axis) in the evolution of the lunar orbit than suggested by the shape solutions. In this paper we explore an evolutionary scenario that reaches moderately large eccentricities during the epoch indicated by the shape results. A key element of our scenario is that the orbital evolution is coupled to the thermal evolution; in this model large eccentricities can be obtained during the shape epoch and still decay sufficiently to connect to the current configuration of the lunar orbit.

We present a coupled thermal model for the evolution of the lunar orbit. We expect that in a lid decoupled from the mantle by a magma ocean tidal heating will be enhanced in the lid (Peale et al., 1979) and dominate that in the mantle. Here we assume dissipation occurs entirely in the lid and that heat transport in the lid is by conduction and melt migration. The model is limited, and there are many unknown parameters. Our goal is not to explore evolutions for all possible parameters, but to show that a high eccentricity orbital phase passing through the shape solution and consistent with today's orbit can be obtained.

In the next section we review aspects of lunar geochronology. Then we recall the Mignard evolutionary equations, correcting a number of typographical errors. This is followed by a presentation of the dissipative lid thermal model, a discussion of the elastic stability of the shape, and our conclusions. In an Appendix A we present in detail the two-layer model for tidal dissipation developed by Peale and Cassen (1978) in their classic study of tidal dissipation in the Moon, correcting a number of typographical errors and making the results explicit.

2. Geochronology constraints

At the beginning of magma ocean solidification the iron- and magnesium-rich phases crystallizing from the cooling magma sink to the bottom of the magma ocean. When approximately 80% of the lunar magma ocean has solidified, plagioclase will begin to crystallize and float; plagioclase will continue to be added to this flotation crust until the last dregs of the magma ocean solidify (Snyder et al., 1992). The ages of the plagioclase in the anorthosite flotation crust, therefore, could span the range from about 80% solidification to the age when the last plagioclase cools below its closure temperature. Here we stress that though geochronological

* Corresponding author. Address: 54-410 MIT, Cambridge, MA 02139, USA.
E-mail addresses: meyerj@mit.edu (J. Meyer), ltelkins@mit.edu (L. Elkins-Tanton), wisdom@mit.edu (J. Wisdom).

0019-1035/$ - see front matter © 2010 Elsevier Inc. All rights reserved.
doi:10.1016/j.icarus.2010.01.029

anorthosite ages have often been interpreted as recording the time of magma ocean solidification, the two are actually decoupled. Anorthosite begins to form long before the magma ocean is solidified, greatly prolongs the remaining solidification process, and may record ages younger than the time of magma ocean solidification if cooled slowly or reheated later.

The short half-life of the tungsten–hafnium (W–Hf) decay system allows dating of the time of separation of the metallic core of a planet from its silicate mantle. Recent work by Touboul et al. (2007) indicates that both the Moon and Earth differentiated primarily after the W–Hf system was extinct, that is, at 60 −10/+90 Myr or more after solidification of the first Solar System materials. Earlier measurements using the same system lead Yin et al. (2002) to conclude that the giant Moon-forming impact occurred at 29 Myr after Solar System formation.

Using 4.567 Gyr as the formation time of the oldest Solar System materials (Connelly et al., 2008) and both the W–Hf dates described here, the earliest age that the Earth and Moon likely differentiated is between 4.538 and 4.507 Gyr. This age for the putative Moon-forming giant impact marks the beginning of the geochemically-determined timeline of formation and cooling of the Moon.

The oldest surface materials on the Moon are assumed to be the anorthositic highlands, formed by flotation in the lunar magma ocean (Wood et al., 1970; Smith et al., 1970). Though there have been a number of geochronological ages determined using the Sm–Nd system, it has inherent difficulties that are improved upon by using the more precise U–Pb system. Nemchin et al. (2009) dated a single zircon crystal from a lunar crustal breccia and obtained an age of 4.417 ± 0.06 Gyr. This zircon was likely the product of crystallization of a small pocket of melt, and implies that this portion of the crust recorded an age of 90–121 Myr after lunar formation.

Planets with a magma surface should cool extremely quickly (Abe, 1993, 1997; Elkins-Tanton, 2008). A plagioclase flotation crust will slow the cooling of the planet significantly in comparison to the cooling of a magma ocean with a liquid surface. Calculations based on techniques from Elkins-Tanton (2008) indicate that the lunar magma ocean may have solidified to 80% in less than 10^4 years, and perhaps as little as 10^3 years. After this near-instantaneous interval plagioclase will begin to form and float. Once sufficient anorthosite has floated to cover the surface of the Moon, cooling will slow substantially; conductive heat loss through the anorthosite lid is the rate-limiting step in cooling.

The anorthosite will record the age at which it cooled past its closure temperature. When the minerals making up the lid are heated, they are prone to losing their radiogenic daughter products through increased diffusion. The closure temperature below which radiogenic ages are preserved through lack of diffusion depends upon mineral type, mineral composition, cooling rate, and absolute temperature. Zircon would lose its original lead composition when subjected to moderate thermal events, on the order of 1000 °C, for even short periods. A 0.1 mm zircon that is heated to 1000 °C for 20,000 years will lose its lead and be geochronologically reset (Cherniak and Watson, 2003). Therefore, no matter when the anorthosite originally formed, if it remains hot or is again heated, the age will record that event. The mineral geochronology is effectively measuring the time of cooling of the tidally heated lid, and not its time of formation.

3. The orbital and rotational model

Mignard (1979–1981) has derived approximate averaged equations governing the evolution of the lunar eccentricity and inclination. The equations of motion are averaged over the orbital period and the period of precession of the lunar orbit. Solar perturbations are included. We use these here, but we allow the relative amount of dissipation in the Moon to that in the Earth (the Mignard A parameter) to change with the thermal state of the Moon.

The Mignard evolutionary equations are:

$$\frac{dX}{dt} = \frac{C_X}{X^7}\left[-\frac{f_0}{\beta^{15}}(1+A) + \left(UX^{3/2}\cos i + A\frac{\omega'}{n}\cos(I')\right)\frac{f_1}{\beta^{12}}\right] \tag{1}$$

$$\frac{de}{dt} = \frac{C_e}{X^8}\left[-\frac{f_3}{\beta^{13}}(1+A) + \left(UX^{3/2}\cos i + A\frac{\omega'}{n}\cos(I')\right)\frac{f_4}{\beta^{10}}\right] \tag{2}$$

$$\frac{di}{dt} = -\frac{C_i}{X^{13/2}}\sin i\left(U + \frac{A}{X^{3/2}}\right)\frac{f_2}{\beta^{10}} \tag{3}$$

$$\frac{dU}{dt} = -C_{U,0}\left[U - \frac{n_\odot}{n_G}\right] + C_{U,1}\frac{1}{X^{15/2}}\left[\frac{f_1}{\beta^{12}} - UX^{3/2}\cos i\frac{f_2}{\beta^9}\right]\cos i - C_{U,2}U(\sin i)^2\frac{1}{X^6}\frac{f_2}{\beta^9} \tag{4}$$

$$\frac{d(\omega/n_G)}{dt} = \frac{C_{\omega,0}}{X^6}\left[-\frac{f_2}{\beta^9}\left[\left(\frac{\omega}{n_G}\right)^2\frac{2+(\sin i)^2}{2} + U^2\frac{3(\cos i)^2-1}{2}\right] + 2U\cos i\frac{f_1}{\beta^{12}}\frac{1}{X^{3/2}}\right] + C_{\omega,1}\left[2\frac{n_\odot}{n_G}U - \left(\frac{\omega}{n_G}\right)^2 - U^2\right] \tag{5}$$

where $\beta = \sqrt{1-e^2}$, $U = (\omega/n_G)\cos(I)$, the grazing mean motion $n_G = \sqrt{GM/R_E^3}$, G is Newton's constant, $X = a/R_E$, with R_E the radius of the Earth, a is the semimajor axis of the lunar orbit, e the orbital eccentricity, n is the orbital mean motion, i is the orbital inclination to the ecliptic, I is obliquity, ω is rotation rate, m is the mass of the Moon, M is the mass of the Earth, $\mu = (1/m + 1/M)^{-1}$ is the reduced mass, and unless otherwise stated primed variables refer to the Moon and unprimed variables refer to the Earth. We also define

$$C_X = 6\gamma\frac{m}{M}\frac{m}{\mu} \tag{6}$$

$$C_e = 3\gamma\frac{m}{M}\frac{m}{\mu} \tag{7}$$

$$C_i = \frac{3}{2}\frac{\gamma}{\alpha}\left(\frac{m}{M}\right)^2 \tag{8}$$

$$C_{U,0} = 3\frac{\gamma}{\alpha}\left(\frac{M_\odot}{M}\right)^2\left(\frac{R_E}{a_E}\right)^6 \tag{9}$$

$$C_{U,1} = 3\frac{\gamma}{\alpha}\left(\frac{m}{\mu}\right)^{1/2}\left(\frac{m}{M}\right)^2 \tag{10}$$

$$C_{U,2} = \frac{3}{2}\frac{\gamma}{\alpha}\left(\frac{m}{M}\right)^2 \tag{11}$$

$$C_{\omega,0} = 3\frac{\gamma}{\alpha}\left(\frac{m}{M}\right)^2\frac{m}{\mu} \tag{12}$$

$$C_{\omega,1} = 3\frac{\gamma}{\alpha}\frac{m}{\mu}\left(\frac{M_\odot}{M}\right)^2\left(\frac{R_E}{a_E}\right)^6 \tag{13}$$

where $\gamma = k_2 n^2 \Delta t$

$$f_0(e) = 1 + \frac{31}{2}e^2 + \frac{255}{8}e^4 + \frac{185}{16}e^6 + \frac{25}{64}e^8$$

$$f_1(e) = 1 + \frac{15}{2}e^2 + \frac{45}{8}e^4 + \frac{5}{16}e^6$$

$$f_2(e) = 1 + 3e^2 + \frac{3}{8}e^4 \tag{14}$$

$$f_3(e) = 9e + \frac{135}{4}e^3 + \frac{135}{8}e^5 + \frac{45}{64}e^7 \tag{15}$$

$$f_4(e) = \frac{11}{2}e + \frac{33}{4}e^3 + \frac{11}{16}e^5 \tag{16}$$

and

$$A = \frac{k_2'}{k_2}\frac{\Delta t'}{\Delta t}\left(\frac{M}{m}\right)^2\left(\frac{R}{R_E}\right)^5 = \frac{k_2'}{Q'}\frac{Q}{k_2}\left(\frac{M}{m}\right)^2\left(\frac{R}{R_E}\right)^5 \tag{17}$$

is a measure of the relative amount of dissipation in the Moon to the dissipation in the Earth, where k_2 is the potential Love number, Q is the tidal dissipation factor, and R is the radius of the Moon, 1738 km. The moment of inertia ratio for the Earth is $\alpha = C_E/\left(MR_E^2\right)$. We take $\alpha = 0.33$.

The Mignard model is limited. The doubly averaged equations cannot follow the precession of the lunar orbit. Furthermore, they use only a single tidal model (the constant Δt Mignard model). The current Moon laser ranging results indicate that the frequency dependence of tidal dissipation might be better described by a more complicated model (Efroimsky and Williams, 2009). However, the physical state of the Earth and Moon in the situation under consideration is so different than at present it is not clear that the same frequency dependence would apply. We assume here that Q is temperature dependent, but ignore possible frequency dependence. A more complicated model does not seem warranted.

The obliquity of the Moon varies substantially as the orbit evolves (Ward, 1975; Wisdom, 2006); in particular large obliquities are obtained during the "Cassini transition" at around $a = 33R_E$, and the rate of tidal dissipation depends on the obliquity (Peale and Cassen, 1978; Wisdom, 2008). However, Peale and Cassen (1978) showed that the tidal heating due to the high obliquities during the Cassini transition did not substantially affect the thermal evolution of the Moon. Here, we are focusing on an earlier epoch during which the obliquity is likely to be close to zero. We take the lunar obliquity $I' = 0$ throughout the evolution.

In our simplified model we assume that the Mignard A parameter varies primarily due to variation in the k_2/Q of the Moon. This assumes that the change in dissipation in the Moon dominates that in the Earth. The reason for this is that the Moon has a lid, which makes the magma ocean last longer than that of the Earth. We define

$$A = C_A(k_2'/Q') \tag{18}$$

where $C_A = A_0/(k_2'/Q')_0$, where A_0 and $(k_2'/Q')_0$ are the initial values of these parameters.

The current value of the A parameter is about 0.3 (Williams et al., 2001), but the value of A early in the evolution of the Earth–Moon system is very uncertain. The Q of the Earth is currently dominated by the Earth's oceans; the Earth's solid body Q is estimated to be 280 (Ray et al., 2001). But the Q of the early Earth, which may have had a magma ocean, may be very different—perhaps ranging from 1 to 300. The k_2 of the early Earth might be more like the fluid Love number of the Earth (0.97) than its current value (0.299). The Q of the Moon has similar uncertainties—perhaps also ranging from 1 to 300. The k_2 of the Moon is presently dominated by rigidity (0.025); the k_2 of an early Moon might be closer to the fluid value of 3/2 for a homogeneous fluid body. Taking account of these uncertainties, the A parameter appropriate for the early Earth–Moon system might range from roughly $0.01 < A < 1000$. We will focus on an initial A parameter of about 1.0, roughly in the middle of this range. For larger values of A_0 the eccentricity plummets to values that are not easy to reconcile with the current eccentricity; for smaller values of A_0 the eccentricity does not get low enough.

The initial rotation state of the Moon is not known. Here we consider only the possibilities that the Moon's rotation was initially synchronous or initially nonsynchronous and asymptotic (Peale and Gold, 1965; Hut, 1981). We did not explore an initial 3:2 rotation state, because we think the synchronous solution is more plausible. For the 3:2 solution one must satisfactorily explain how the Moon was captured into the resonance and then explain how it escaped. For a constant Δt (Mignard) tidal model, the expression for the asymptotic rotation rate is (Levrard et al., 2007)

$$\frac{\omega'}{n} = \frac{N(e)}{\Omega(e)}\frac{2x}{1+x^2} \tag{19}$$

where $x = \cos I'$, for the obliquity of the Moon I', $N(e) = f_1(e)/\beta^{12}$, and $\Omega(e) = f_2(e)/\beta^9$. If the Moon's initial rotation was nonsynchronous and asymptotic, then when the Moon's rotation rate is close enough to synchronous the rotation rate becomes locked to synchronous. Here we assume that locking occurs if

$$\left|\frac{\omega'}{n} - 1\right| < \frac{5}{8}\epsilon \tag{20}$$

where $\epsilon = (3(B-A)/C)^{1/2}$ is the out-of-roundness parameter, and $A < B < C$ are the principal moments of inertia of the Moon. We do not know the value of ϵ when capture might have occurred; here we take the critical $(5/8)\epsilon$ to be 0.01. The evolution is not sensitive to this choice, because once the eccentricity begins to decrease, it decreases rapidly to small values.

The initial eccentricity of the Moon is also unknown. We presume here that the Moon formed from a giant impact with the Earth, and that the Moon formed roughly in the equatorial plane of the Earth with only moderate eccentricity. The Moon-forming n-body simulations of Kokubo et al. (2000) found that the eccentricity of the initial lunar orbit ranged from 0.00 to 0.15. We think that these results should not be taken too literally since the physical state of the Moon-forming disk is not likely to be well represented by a collection of cold point particles. Instead it is likely that the Moon-forming disk was largely molten (Thompson and Stevenson, 1988), and that the Moon formed from cooler material being lost from the outer edge of the disk. But the formation of the Moon in this scenario has not been studied, so there are no other hints as to the initial eccentricity of the lunar orbit. Another process may play a role in setting the initial orbital eccentricity: passage through the evection resonance. Even if the dance of the lunar orbit through the evection and eviction resonances as described in Touma and Wisdom (1998) does not occur (perhaps because the rate of tidal evolution is too large for capture to occur) it is likely that the eccentricity will suffer a non-adiabatic change on passing through the strong evection resonance. Touma and Wisdom (1998) found non-adiabatic eccentricities from 0.00 to 0.08 in this case. We assume $e = 0.05$ at $X = a/R_E = 6$, initially. We assume the initial inclination at this point is 10°, the initial rotation period of the Earth is 5 h, and the initial obliquity of the Earth is 10° (Touma and Wisdom, 1994).

4. The dissipative lid model

The model Moon consists of a plagioclase lid with initial thickness 10 km, above a magma ocean with initial thickness 200 km, above a solid interior. We assume that the magma ocean is convecting and the adiabatic temperature profile is characterized by a constant temperature T_f (the temperature at the top of the magma ocean). We take the initial value $T_f = 1573$ K. Tidal heating occurs solely in the lid and the temperature profile of the lid is modeled. The temperature at the surface of the lid is fixed at the equilibrium temperature, assumed to be 280 K. The temperature at the base of the lid is fixed to match the temperature of the magma ocean, T_f. We assume an initial thermal profile that is linear between these two values. The temperature profile in the lid evolves according to Fourier's law of heat conduction. As the temperatures in the interior of the lid evolve to above the solidus of plagioclase, heat is advected to the layers above by rising plagioclase liquid. The solidus of plagioclase is assumed to be $T_p = 1823$ K (Deer et al., 1996).

The thermal evolution in the lid is described by

$$\frac{\partial T}{\partial t} = \frac{2\kappa}{r}\frac{\partial T}{\partial r} + \frac{\partial}{\partial r}\left(\kappa\frac{\partial T}{\partial r}\right) + \frac{H}{\rho_l C_p} + \left.\frac{\partial T}{\partial t}\right|_{melt} \tag{21}$$

where r is the radius and t is the time, H is the local volumetric tidal heating rate, $\kappa = k/(\rho_l C_p)$ is the thermal diffusivity, C_p is the specific

heat capacity, and k is the thermal conductivity. The density in the lid ρ_l is 2730 kg/m^3. We use $C_p = 1256$ J kg^{-1} K^{-1} and $\kappa = 10^{-6}$ m^2 s^{-1}. This equation is just Fourier's law written in spherical coordinates, with the approximation that the heating and temperature are spherically symmetric (do not depend on angles).

The tidal heating rate in a homogeneous satellite at arbitrary eccentricity and obliquity was determined by Wisdom (2008). There it was shown that the tidal heating at large eccentricity can be dramatically larger than the conventional (e^2) formula gives. That calculation assumes a specific tidal model, where the tidal bulge is delayed by a constant time lag (the Mignard model). For other tidal models presumably the form of the dissipation is somewhat different, but considering other uncertainties this form should be adequate. The heating rate is

$$\left.\frac{dE}{dt}\right|_{Tidal} = \frac{21}{2}\frac{k_2}{Q}\frac{GM^2R^5n}{a^6}\zeta(e,I') \tag{22}$$

where k_2 and Q are the satellite's potential Love number and tidal dissipation factors, respectively, M is the mass of the Earth, R is the radius of the (homogeneous) Moon, n is the orbital mean motion, a is the semimajor axis of the orbit, e is the orbital eccentricity, I' is the obliquity of the satellite to the orbit, and

$$\zeta(e,I') = \frac{2}{7}\frac{f_0(e)}{\beta^{15}} - \frac{4}{7}\frac{f_1(e)}{\beta^{12}}\cos I' + \frac{1}{7}\frac{f_2(e)}{\beta^9}(1+(\cos I')^2) \tag{23}$$

where $\beta = (1-e^2)^{1/2}$.

We use the two-layer model from Peale and Cassen (1978) described and corrected in Appendix A to estimate the tidal heating as a function of radius in the lid. The local heating rate, averaged over angles, is given by:

$$H = \frac{\mu_L G^2M^2k_2^2R^2n\zeta(e,I')}{a^6Qg^2}\left(-126(\alpha_1')^2 + \frac{252}{5}\alpha_1'\alpha_2' - \frac{42}{5}(\alpha_2')^2 - \frac{21}{5}(\alpha_0')^2 - \frac{252}{5}(\alpha_3')^2\right) \tag{24}$$

where the surface acceleration on the Moon is $g = 1.62$ m s^{-2} and, where μ_L is the rigidity of the lid, which we assume constant. We use 6.5×10^9 N m^{-2}. This is a factor of 10 smaller than that used by Peale and Cassen (1978) based on seismic velocities in today's cold Moon; we use a lower rigidity because of the high temperatures in the lid during the early epoch. To some extent the choice of rigidity is arbitrary and offset by the uncertainty in the values of the tidal Qs of the early Earth and Moon. The temperature dependence of the rigidity of the plagioclase lid is ignored and the α_i' and k_2 functions are given in Appendix A.

The lid is varying in thickness δ_l and we parameterize depth in the lid using y which varies from 0 (at the surface) to 1 (at the base). Let $T(t,r) = T'(t,y)$, with $r = R - \delta_l y$, where R is the radius of the Moon, then the heat equation becomes

$$\frac{\partial T'}{\partial t} = -\frac{2\kappa}{\delta_l r}\frac{\partial T'}{\partial y} + \frac{\kappa}{\delta_l^2}\frac{\partial^2 T'}{\partial y^2} + \frac{\partial T'}{\partial y}\frac{y\dot{\delta}_l}{\delta_l} + \frac{H}{\rho_l C_p} + \left.\frac{\partial T'}{\partial t}\right|_{melt} \tag{25}$$

We introduce a discretization of the lid by dividing it into N spherical shells of thickness $\Delta r = \delta_l \Delta y$. Let T^i be the temperature in the ith shell corresponding to $y^i = i\Delta y$, where i runs from 0 at the surface to N at the base of the lid. Then Eq. (25) becomes

$$\frac{dT^i}{dt} = -\frac{2\kappa}{\delta_l r}\left(\frac{T^{i+1}-T^{i-1}}{2\Delta y}\right) + \frac{\kappa}{\delta_l^2}\left(\frac{T^{i+1}-2T^i+T^{i-1}}{\Delta y^2}\right) + \left(\frac{T^{i+1}-T^{i-1}}{2\Delta y}\right)\frac{y\dot{\delta}_l}{\delta_l} + \frac{H}{\rho_l C_p} \tag{26}$$

The melt migration term is handled separately.

As layers of the lid reach their melting temperature, portions of these layers begin to melt as heat continues to be added. The amount of melt mass depends on the latent heat of melting, $L = 5\times10^5$ J/kg. These melted portions rise to the surface, due to their positive buoyancy, bringing heat and mass with them. We model the ascent of this melt using a leaky dike model, where the melt loses a fraction of its heat and mass to each layer that it rises through. We varied the leak fraction from 0 to 1. The qualitative behavior is insensitive to this parameter; for the runs reported here we use 0.02 (for $N = 100$). Any heat remaining when the melt reaches the surface is assumed to be instantaneously radiated away. The remaining mass is deposited at the surface and the layers are redefined to account for the new mass distribution. As the melt is removed from a layer and redeposited in other layers or at the surface, the layers are redefined so that they remain equal in mass to the original layers. The temperature of the redefined layer is the mass-weighted average of the temperatures of the original layers that were incorporated into each layer.

The thermal evolution of the magma ocean is described by two equations. First,

$$4\pi(R-\delta_l)^2 k\left.\frac{dT}{dr}\right|_{base} + \dot{E}_r = -4\pi(R-\delta_l)^2 k\frac{1}{\delta_l}\left.\frac{dT}{dy}\right|_{base} + \dot{E}_r = C_p\rho_f(\dot{V}_f T_f + \dot{T}_f V_f) \tag{27}$$

where the left-hand side is heat conducted out of the magma ocean into the lid plus radiogenic heating $\dot{E}_r$, and the right-hand side is the change in heat content as a result of changing the volume V_f by both melting/freezing and changing the temperature in the magma ocean. We take $\rho_f = 3000$ kg m^{-3}. We compute the radiogenic heating by extrapolating the chondritic abundances of ^{235}U, ^{238}U, ^{40}K, and ^{232}Th back to the time of formation of the Moon. We then multiply by the heat production per mass, the density, and the volume of the magma ocean and sum over the four isotopes. The half-lives, current abundances, and specific heat productions are given by Turcotte and Schubert (2002).

Second,

$$\frac{\dot{T}_f}{T_{sol}}f = -\frac{\dot{V}_l}{V_{fi}} = -4\pi(R-\delta_l)^2\frac{\dot{\delta}_l}{V_{fi}} \tag{28}$$

which describes the fractional crystallization of the magma ocean. Here V_f is the volume of the magma ocean and V_l is the volume of the lid. We are assuming fractional solidification is linear between the magma ocean solidus and liquidus. Here, $T_{sol} = T_{fi} - T_s$ is the difference between the initial temperature in the magma ocean and the solidus, and V_{fi} is the initial volume of the magma ocean. Each fractional increment in temperature change between those values, $\Delta T_f/T_{sol}$, results in a similar fractional change in the solid to liquid ratio of the magma ocean $\Delta V_f/V_{fi}$. The factor f is the proportion of plagioclase in the solidified portion of the melt; this is added to the base of the lid. We assume $f = 0.2$ (Snyder et al., 1992; Warren, 1986). As the magma ocean crystallizes, f gives the fraction of material that joins the lid and $1-f$ gives the fraction that joins the solid interior at the base of the magma ocean.

The solidus of the fractionally solidifying magma ocean, T_s, is parameterized to fit the bulk lunar mantle solidus of Longhi (2003). As crystallization proceeds and solidification moves to shallower depths, the solidus moves to lower temperatures than the Longhi (2003) results as the remaining liquid composition evolves. This evolution is expressed in the final term of the solidus expression, calibrated to match temperatures calculated from the MELTS program (Ghiorso and Sack, 1995). We use

$$T_s = 2134 - 0.1724\epsilon - 1.3714\times10^{-4}\epsilon^2 - \frac{4.4}{0.2V_f/V_{fi}+0.01} \tag{29}$$

where T_s is the solidus in Kelvin and ϵ is the radius of the base of the lid in kilometer.

The change in magma ocean depth δ_f can be related to the change in lid thickness using $\dot{V}_l = -f\dot{V}_f$:

$$\dot{\delta}_f = \frac{(1-1/f)(R-\delta_l)^2 - (R-\delta_l-\delta_f)^2}{(R-\delta_l-\delta_f)^2}\dot{\delta}_l = A_1\dot{\delta}_l. \tag{30}$$

Then we can relate the rate of change in magma ocean volume $\dot{V}_f$ to the rate of change of the lid thickness $\dot{\delta}_l$. The volume of the magma ocean is

$$V_f = \frac{4}{3}\pi(R-\delta_l)^3 - \frac{4}{3}\pi(R-\delta_l-\delta_f)^3 \tag{31}$$

and so

$$\dot{V}_f = -4\pi(R-\delta_l)^2\dot{\delta}_l + 4\pi(R-\delta_l-\delta_f)^2(\dot{\delta}_l+\dot{\delta}_f) = A_2\dot{\delta}_l + A_3\dot{\delta}_f \tag{32}$$

Solving the above equations, we find that

$$\dot{\delta}_l = \frac{-4\pi(R-\delta_l)^2\kappa\frac{1}{\delta_l}\frac{dT}{dy}\Big|_{base} + \dot{E}_r}{-4\pi(1/f)(V_f/V_{fi})(R-\delta_l)^2T_{sol} + T_f(A_2+A_1A_3)} \tag{33}$$

and

$$\dot{T}_f = -\frac{T_{sol}}{f}\frac{4\pi(R-\delta_l)^2}{V_{fi}}\dot{\delta}_l \tag{34}$$

Upon discretization, Eq. (33) becomes

$$\dot{\delta}_l = \frac{-4\pi(R-\delta_l)^2\kappa(T^{N-1}-T^{N-2})/(\Delta y\delta_l) + \dot{E}_r}{-4\pi(1/f)(V_f/V_{fi})(R-\delta_l)^2T_{sol} + T_f(A_2+A_1A_3)} \tag{35}$$

We choose an effective $1/Q$ of the lid by averaging the $1/Q$ of the individual layers, as given in terms of the temperature of each layer by the Ojakangas–Stevenson formula,

$$\frac{1}{Q}(T_i) = \frac{1}{Q_{max}} + \left[\frac{1}{Q_{min}} - \frac{1}{Q_{max}}\right]\left(\frac{T_i}{T_p}\right)^n \tag{36}$$

We set $Q_{max} = 100$, and let Q_{min} vary with the run. Experimentally, the parameter n ranges from 20 to 30 (Ojakangas and Stevenson, 1986); we use 25. We integrate Eqs. (26) and (35) as well as the equations for $\dot{\delta}_f$ and $\dot{T}_f$ using the Bulirsch–Stoer algorithm, which has automatic step-size control. We carry out melt migration every 1 year. In our simulations we usually set the number of layers $N = 100$, but varied this parameter (and the corresponding leak fraction) to check that our results were insensitive to it.

Fig. 1 shows the eccentricity of the lunar orbit versus the semimajor axis for a run in which $A_0 = 1.0$, the Earth's phase lag $\Delta t = 123$ min (with $k_2 = 0.97$), and the lunar $Q_{min} = 0.35$. These parameters were chosen to give a peak eccentricity near that required by the shape solution. There is considerable flexibility in the peak eccentricity; generally, increasing the dissipation in the Earth (larger Δt) gives a larger e_{max}, but this must be compensated by a smaller Q_{min} to match the current eccentricity of the lunar orbit. A more complete model would allow the Earth's k_2 and Q to vary with time, and would probably give different constraints on Q_{min} for the Moon. Thus the very low value of Q_{min} should not be taken too seriously. We reduced Δt to 2.6 min (with $k_2 = 0.299$) when the orbit reached $30R_E$ to approximate the changes in these parameters, and so that the evolution to $60R_E$ would take about 4.6 Gyr.

Fig. 2 shows the tidal heating in the lid and compares it to the radiogenic heating in the magma ocean. Tidal heating peaks when the eccentricity is at a maximum and remains higher than the radiogenic heating rate until the eccentricity becomes small.

Fig. 3 shows the evolution of the depth of the lid and the depth of the magma ocean as a function of time. In this model, the magma ocean solidifies at 272 Myr. The lid reaches a final thickness of 46 km. Radiogenic heating prolongs the magma ocean by about 55 Myr.

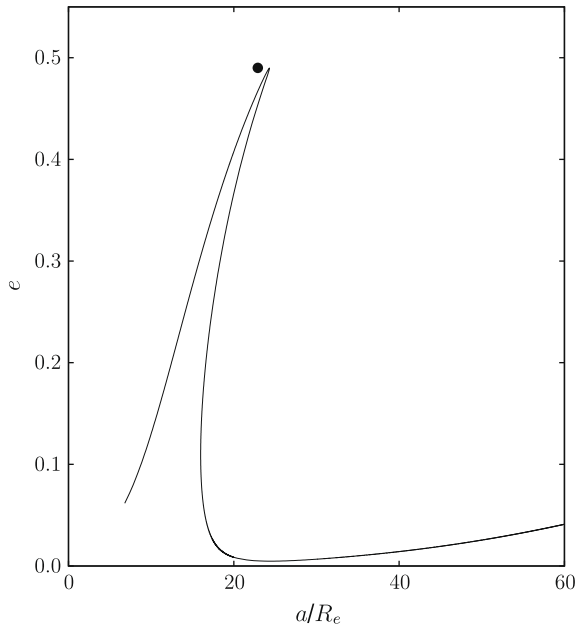

Fig. 1. The eccentricity of the lunar orbit plotted versus the semimajor axis of the orbit, for the dissipative lid model. For reference, the dot shows the orbit that gives the solution to the shape problem for synchronous rotation.

Fig. 4 shows the temperature at four layers in the lid versus the logarithm of the time for this same run. The temperature at 10 km depth decreases below the closure temperature of 1000 °C for zircons (Cherniak and Watson, 2003) at a time of about 9.1 Myr, at 15 km depth at a time of 32.5 Myr, at 20 km depth at a time of 63.2 Myr, at 25 km depth at a time of 100.2 Myr, and at 30 km depth at a time of 142.0 Myr. Our model cannot follow the temperatures in the lid once the magma ocean solidifies, so the graphs of the temperatures are terminated at this point. As discussed above, the closure time needs to be 90–121 Myr after lunar formation to

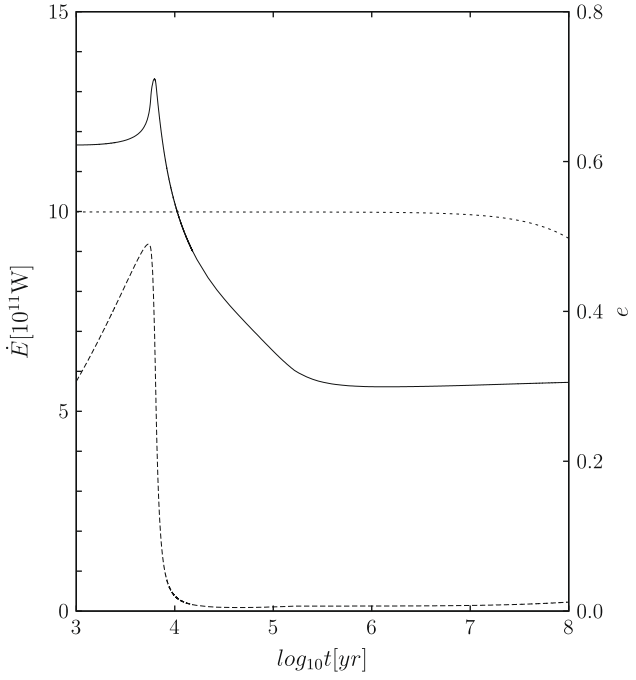

Fig. 2. The tidal heating rate in the lid plotted versus time (solid line, see left axis). The radiogenic heating rate in the magma ocean is shown as a dotted line. The dashed line shows the orbital eccentricity versus time (see right axis).

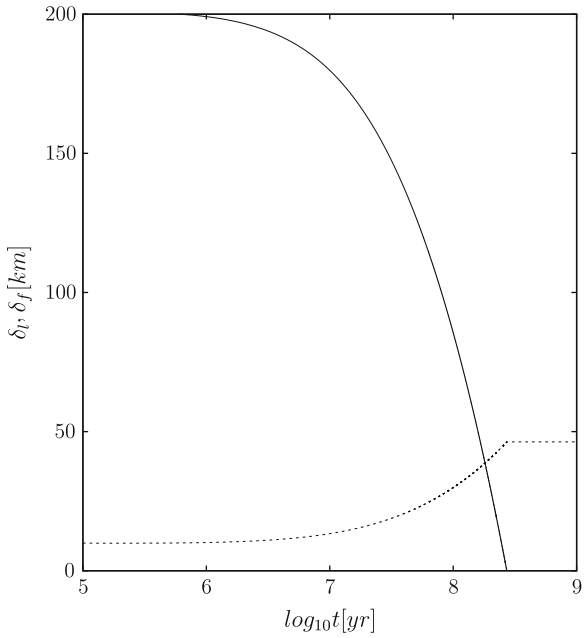

Fig. 3. The depth of the magma ocean δ_f (solid) and the depth of the lid δ_l (dotted), plotted versus the logarithm of the time, for the dissipative lid model. In this model the magma ocean disappears after about 217 Myr, and the lid reaches its full depth of about 46.3 km.

match the zircon dates. Our model suggests that the dated zircon originates from a depth of approximately 25 km.

Fig. 5 shows the temperature at four layers in the lid versus the logarithm of the time for a run in which the eccentricity and consequently the tidal heating has been set to zero. The thermal evolution is decoupled from the orbital evolution. We see that tidal heating affects the temperature of the shallowest layer, but not at depth. Thus even without tidal heating the dated zircon must originate at a depth of approximately 25. So the geochronology is consistent with our model if we focus on closure times at depth instead of solidification times of surface materials. Therefore, the age of the lunar breccias is not evidence for a high eccentricity phase of the lunar orbit.

5. Elastic stability of the shape solution

We have found that a high eccentricity phase of lunar evolution can carry the Moon through the synchronous shape solution. But in our model, and likely any model, the temperatures in the lid are close to a peak during this phase. So for the shape to record this high eccentricity phase, in our model we must rely on the rapid freezing of the melt as it reaches the surface of the Moon. As a large percentage of the lid is processed as melt during the high eccentricity phase, this may give a way of recording the shape even though tidal heating is also near a peak. Several questions arise, though, concerning the subsequent stability of the shape of this frozen lid. As the orbit continues to evolve to lower eccentricity and larger semimajor axis, the gravitational and centrifugal potentials change and so the lid must develop stress in order to maintain its shape. Is this stress below the breaking stress? Is the lid strong enough so that it can maintain its shape rather than elastically deform to subsequent hydrostatic shapes? We consider these questions in this section.

We follow the method described in Goldreich and Mitchell (2009), Matsuyama and Nimmo (2008), and Vening Meinesz (1947). First, recall (Garrick-Bethell et al., 2006) that the average tidal and centrifugal potential at orbital eccentricity e and semimajor axis a gives rise to a triaxial distortion of the surface of the Moon with the distortions along the principal axes of

$$\Delta r_a = hcR\left(\frac{3}{4}X_{-3,2,2}(e) + \frac{5}{12}\right) \tag{37}$$

$$\Delta r_b = -hcR\left(\frac{3}{4}X_{-3,2,2}(e) - \frac{5}{12}\right) \tag{38}$$

$$\Delta r_c = -hcR\left(\frac{1}{2}X_{-3,0,0}(e) + \frac{1}{3}\right) \tag{39}$$

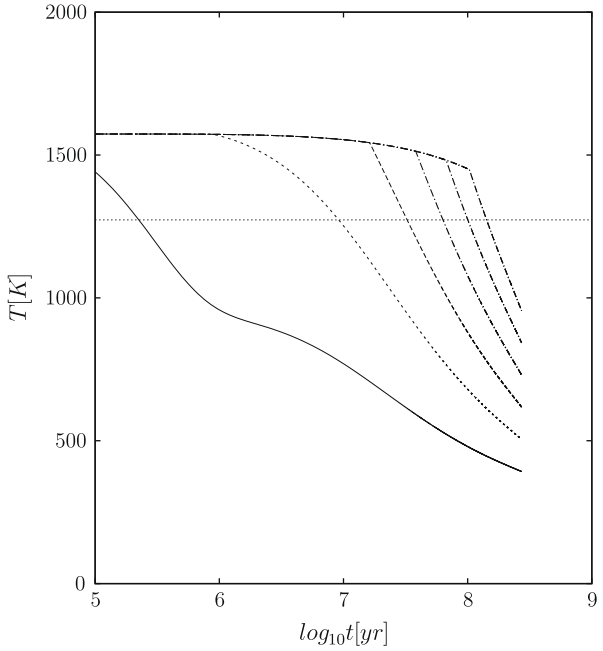

Fig. 4. The temperature at four layers in the lid plotted versus the logarithm of the time, for the dissipative lid model. The eccentricity behavior is as shown in Fig. 1. The depths of each layer are 5 km, 10 km, 15 km, 20 km, 25 km, and 30 km. The temperature increases with depth. The horizontal line indicates the approximate closure temperature of zircon.

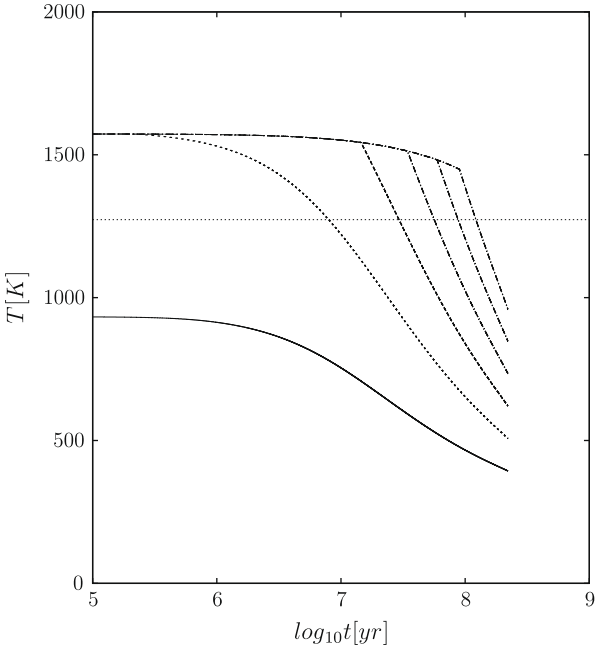

Fig. 5. The temperature at four layers in the lid plotted versus the logarithm of the time, for the dissipative lid model. Here the eccentricity and consequently the tidal heating are set to zero. The depths of each layer are 5 km, 10 km, 15 km, 20 km, 25 km, and 30 km. The temperature increases with depth. The horizontal line indicates the approximate closure temperature of zircon.

where R is the radius of the Moon, $h \approx 5/2$ is the fluid displacement Love number, $X_{i,j,k}$ are Hansen functions (Plummer, 1960), and

$$c = \left(\frac{R}{a}\right)^3 \frac{m_{Earth}}{m_{Moon}} \tag{40}$$

We assume the $\hat{a}$ axis points to the Earth (the Moon rotates synchronously), the $\hat{c}$ axis is perpendicular to the orbit, and the intermediate $\hat{b}$ axis completes a right-hand basis set $(\hat{a}, \hat{b}, \hat{c})$. In terms of these principal displacements we calculate the displacement d of the surface of the rigid lid in terms of the colatitude θ measured from the $\hat{c}$ axis, and the angle γ measured from the $\hat{a}$ axis. (The spherical coordinates are completed by a longitude ϕ measured from the meridian through the $\hat{a}$ axis.) We find

$$d = R\left[\alpha(\cos^2\theta - 1/3) + \beta(\cos^2\gamma - 1/3)\right] \tag{41}$$

with

$$\cos\gamma = \sin\theta\cos\phi \tag{42}$$

and where

$$\alpha R = \Delta r_c - \Delta r_b \tag{43}$$
$$\beta R = \Delta r_a - \Delta r_b \tag{44}$$

In terms of these, we can express the surface stresses:

$$\sigma_{\theta\theta} = \mathscr{A}\mu\left[\Delta\alpha\ (3\cos^2\theta + 1) + \Delta\beta\ (3\cos^2\phi\ (3 - \cos^2\theta) - 5)\right] \tag{45}$$
$$\sigma_{\phi\phi} = \mathscr{A}\mu\left[\Delta\alpha\ (9\cos^2\theta - 5) + \Delta\beta\ (3\cos^2\phi\ (1 - 3\cos^2\theta) + 1)\right] \tag{46}$$
$$\sigma_{\theta\phi} = \mathscr{A}\mu[\Delta\beta\ (3\cos\theta\sin\phi\cos\phi)] \tag{47}$$

where

$$\mathscr{A} = \frac{2}{3}\left(\frac{1+\nu}{5+\nu}\right) \tag{48}$$

and where μ is the rigidity, and ν is Poisson's ratio, which we take to be 1/4. In these expressions we have written the stress in terms of $\Delta\alpha$ and $\Delta\beta$ which are the differences between α and β at a given orbit (a, e) minus the values of these parameters at the particular orbit given by the shape solution. We assume the stresses are zero at the shape solution. Other components of the stress are zero.

For a rigidity of 5×10^{10} N m^{-2}, the stresses are approximately 1 kbar. This is approximately the breaking stress for the lunar lithosphere (Solomon, 1986). Thus the lithosphere may break, losing its shape. However, the rigidity is likely to be smaller than given because the temperatures are high. So we may be able to avoid breaking.

The Moon could also elastically respond to these stresses by changing its shape. Now we consider whether this is energetically favorable. Once the Moon's orbit has returned to a low eccentricity, the equilibrium shape will be different. If the Moon does not elastically change its shape to match the equilibrium shape, gravitational potential energy will be stored in the frozen-in shape. If the Moon's shape does change, elastic energy will be stored via the additional stresses in the lithosphere. Since the Moon will tend to the lowest energy configuration, we can judge which of these two outcomes will occur by comparing the stored gravitational energy to the stored elastic energy.

The elastic energy density is given by

$$\mathscr{E} = \frac{1}{2}\sum_{ij}\sigma_{ij}u_{ij} = \frac{1}{2}\left(\sigma_{\theta\theta}u_{\theta\theta} + \sigma_{\theta\theta}u_{\phi\phi}\right) + \sigma_{\theta\phi}u_{\theta\phi} \tag{49}$$

where the strains are given by

$$u_{\theta\theta} = \frac{\sigma_{\theta\theta} - \nu\sigma_{\phi\phi}}{2\mu(1+\nu)} \tag{50}$$
$$u_{\phi\phi} = \frac{\sigma_{\phi\phi} - \nu\sigma_{\theta\theta}}{2\mu(1+\nu)} \tag{51}$$
$$u_{\theta\phi} = \frac{\sigma_{\theta\phi}}{2\mu} \tag{52}$$

We integrate over the volume of the lid to find the total elastic energy

$$E_e = \frac{2\pi\delta_l R^2\mu}{1+\nu}\mathscr{A}^2\left[(\Delta\alpha)^2\left(\frac{8}{5}\nu + 8\right) - \Delta\alpha\Delta\beta\left(\frac{8}{5}\nu + 8\right) + (\Delta\beta)^2\left(\frac{19}{40}\nu + \frac{55}{8}\right)\right] \tag{53}$$

Next we compute the gravitational energy. The energy is

$$E_g = \int_V \overline{U}_T\rho r^2\sin\theta\, dr\, d\theta\, d\phi, \tag{54}$$

where V is the volume of the Moon, and the average tidal potential is

$$\overline{U}_T(r,\theta,\phi) = n^2 r^2 \widetilde{U}_T(\theta,\phi) \tag{55}$$

We find

$$\widetilde{U}_T(\theta,\phi) = B_2(e)P_2(\cos\theta) + B_{2,2}(e)P_{2,2}(\cos\theta)\cos 2\phi, \tag{56}$$

where $P_2(x) = (3/2)x^2 - 1/2$ and $P_{2,2}(x) = 3(1-x^2)$ and

$$B_2(e) = \frac{1}{2} + \frac{1}{3}X_{-3,0,0}(e) \tag{57}$$
$$B_{2,2}(e) = -\frac{3}{2}X_{-3,2,2}(e) \tag{58}$$

The Hansen coefficients are

$$X_{-3,2,2}(e) = 1 - \frac{5}{2}e^2 + \frac{13}{16}e^4 - \frac{35}{288}e^6 + \cdots \tag{59}$$
$$X_{-3,0,0}(e) = (1-e^2)^{-3/2} \tag{60}$$

To compute the volume integral we make a change of variables from r to s

$$r = s(R + d(\theta,\phi)) \tag{61}$$

to get

$$E_g = n^2\rho\int_0^1 ds\int_0^\pi d\theta\int_0^{2\pi} d\phi\left[\widetilde{U}_T(\theta,\phi)s^4(R + d(\theta,\phi))^5\sin\theta\right] \tag{62}$$
$$= n^2\rho R^4\int_0^\pi d\theta\int_0^{2\pi} d\phi\left[d(\theta,\phi)\widetilde{U}_T(\theta,\phi)\sin\theta\right] \tag{63}$$

where we have made a small d/R approximation, and used the fact that the angular integral of $\widetilde{U}_T$ is zero. Next using

$$d(\theta,\phi) = -h\frac{\overline{U}_T(R,\theta,\phi)}{g_{Moon}} = -\frac{hn^2R^2}{g_{Moon}}\widetilde{U}_T(\theta,\phi) \tag{64}$$

then

$$E_g = -\frac{n^4\rho h R^6}{g_{Moon}}\int_0^\pi d\theta\int_0^{2\pi} d\phi\left[(\widetilde{U}_T(\theta,\phi))^2\sin\theta\right] \tag{65}$$
$$= -hcm_{Moon}n^2R^2\frac{3}{4\pi}\left[\frac{2}{5}(B_2(e))^2 + \frac{24}{5}(B_{2,2}(e))^2\right] \tag{66}$$

We compute the difference in the elastic energy from the stress-free shape solution $a = 22.9R_E$, $e = 0.49$, to the elastic energy at $a = 22.9R_e$, $e = 0.0$, and similarly for the gravitational energies. Using $\mu = 5 \times 10^{10}$ Pa, $n = 1.35 \times 10^{-5}$ s^{-1} (for $a \approx 20R_e$), $h = 5/2$,

$\delta_l = 10^4$ m, $m_{Moon} = 7.35 \times 10^{22}$ kg, $c = 1.4 \times 10^{-4}$, we find that the elastic energy stored in going to zero eccentricity is 9.2×10^{19} J. The difference of the gravitational energy between these two orbital configurations is 1.7×10^{21} J. The ratio of the change in elastic energy to the change in the gravitational energy is about 0.053. This implies that the shape will deform elastically and lose memory of the shape solution. This elastic change in shape would be essentially instantaneous compared to the timescales of the evolution we are considering. The stresses that develop would then relax on a viscous timescale, which is very uncertain.

6. Conclusions

We have developed a simplified model for studying the coupled thermal–orbital evolution of the early Moon. The model assumes tidal heating occurs only in the lid and gives a temperature profile of the lid as a function of time. We assume that the variations of the k_2 and Q of the Moon dominate those of the Earth. Future work should include tidal dissipation and heat transfer in both the mantle and the lid, and model the variation in Earth's k_2 and Q.

The eccentricity of the lunar orbit can reach high values in this model. For small dissipation in the Moon (small Mignard A parameter), an initial eccentricity tends to grow. As the eccentricity grows to large values the tidal heating increases dramatically (Wisdom, 2008). This heats the Moon and causes the Q of the Moon to change due to its strong temperature dependence. With a small Q (large A parameter) the Moon's eccentricity begins to decay.

Parameters can be chosen that cause the orbit to pass close to the values of semimajor axis and eccentricity required by the synchronous shape solution of Garrick-Bethell et al. (2006). The parameters we had to choose are somewhat extreme, particularly the Δt of the Earth. Holding other parameters constant, the value of the peak eccentricity is larger for larger dissipation in the Earth (larger Δt). To reach the eccentricity of Garrick-Bethell et al. (2006) we had to use a Δt of 123 min (for $k_2 = 0.97$). On the other hand, it is not known how dissipative the early Earth would have been.

Perhaps a more severe problem is that the orbit matches the shape solution at a time when tidal heating of the plagioclase lid is at its peak. Garrick-Bethell et al. (2006) demonstrated that this shape does indeed match the current shape of the Moon, but whether it could have been preserved after formation at that eccentricity, while the heating rate is large, remains the question.

During the period capable of creating the crustal shape observed on the Moon today, portions of the lunar crust were being melted through tidal dissipative heating, erupted to the surface, and quenched. We find that 89% of the lid is processed as melt in our model. The melt material that is placed on the surface solidifies and cools quickly, and may record the shape of the moon during the time of melt production. The peak of melt production is after the peak eccentricity, so it may be that the recorded shape will reflect a lower eccentricity than the peak. The rigidity of this surface and near-surface crust would be significant.

At the time of melt production, the lid is still underlain by a magma ocean which allows for elastic deformation of the lid. To determine whether the shape would be preserved until the present, we can make a simple energetics argument. If the Moon kept the shape that it froze in at the peak of eccentricity, when the orbit drops to low eccentricity, gravitational potential energy will be stored in the now non-equilibrium shape. If instead the Moon elastically deforms to match the new equilibrium shape, there will be elastic energy stored due to the stresses in the lid. By comparing the elastic and gravitational energies, we determined that the Moon will elastically deform and lose the shape it developed at the peak. So we conclude that if a magma ocean is still present at the high eccentricity phase during which the shape is frozen in (as in our model) then the shape could not be maintained as the orbit evolved to lower eccentricity. If we try to circumvent this conclusion by increasing the rigidity, then we have shown that the lithosphere would break, again losing its shape.

Though the shape cannot be explained by a high eccentricity phase of the evolution of the lunar orbit, a high eccentricity phase is not excluded. The coupled thermal–orbital model presented here can give high eccentricities which subsequently damp to values low enough to reach the present eccentricity (whether or not some component of the lunar eccentricity is due to passage through the Jovian evection resonance).

At the peak of tidal heating the crust is melted internally and molten anorthosite erupted onto the lunar surface. These materials will cool quickly, so the closure age is roughly the same as the age of crystallization, which is less than 1 Myr after lunar formation. This short time lag is insufficient to explain the young ages measured in lunar rocks.

At depth in the crust materials will have their geochronological ages reset by heating over a far longer time period than the period of active melting. The crust is heated to temperatures below melting but above the zircon closure temperature of 1000 °C (Cherniak and Watson, 2003). If the lunar breccias originate at a range of depths, they will experience varying delays in cooling that could explain the range of ages measured. For the sample dated by Nemchin et al. (2009), we find that an origin at about 25 km depth is consistent with the measured age.

The lunar crust is highly brecciated from impacts, and rocks used for age determination may have originated at depth and been excavated by impacts. Wieczorek and Phillips (1999) estimates that the original excavation depths of the major basins range from 15 to 50 km, making the scenario of mid-crustal origin for these rocks plausible. The zircon dated by Nemchin et al. (2009) is from a melt breccia, sample 72215, and its depth of origin is unknown. However, Garrick-Bethell et al. (2009) demonstrated that sample 76535 was excavated from a depth of about 45 km without being brecciated or melted. This is further evidence that the dated zircon could have originated at large depth.

We find that an early high eccentricity phase of the lunar orbit is a robust feature of our model. Though the high eccentricity orbit passes through the synchronous shape solution, we conclude that it is unlikely that the Moon's shape during this epoch could persist to the present. Lunar geochronology of crustal breccias can be explained if they originate at depth.

Acknowledgments

We thank Bill McKinnon, Jonathan Mitchell, Francis Nimmo, Stan Peale, Darin Ragozzine, Dave Stevenson, Ben Weiss, and Maria Zuber for helpful conversations.

Appendix A. Tidal heating in a two-layer model

In a classic paper Peale and Cassen (1978) calculated the rate and distribution of tidal dissipation in the Moon. They also calculated the rate of tidal heating in a two-layer model, consisting of an inviscid molten interior overlain by a rigid lid. The result was used in another classic paper, Peale et al. (1979), in which it was predicted that there would be volcanoes on Io. We set out to use the two layer model, but found that there were a number of typographical errors, and that a considerable amount of work was required to recover explicit expressions for the local energy dissipation. So the result of our labor is presented here.

The two-layer model consists of an inviscid fluid interior overlain by a rigid lid. The lid has rigidity μ, density ρ, and surface gravity g. The radius of the satellite is R, G is Newton's constant, a is the semimajor axis of the orbit, e is orbital eccentricity, and n is orbital

mean motion. The radius of the interior divided by the radius of the satellite is η.

Let

$$A(a,b) = (a(1+\eta+\eta^2) + b(\eta^3+\eta^4))/E \tag{67}$$

$$B(c,d) = (c(1+\eta+\eta^2+\eta^3+\eta^4) + d(\eta^5+\eta^6))/E \tag{68}$$

$$C(e,f) = (e(\eta^3+\eta^4) + f(\eta^5+\eta^6+\eta^7+\eta^8+\eta^9))/E \tag{69}$$

$$D(g,h) = (g(\eta^5+\eta^6) + h(\eta^7+\eta^8+\eta^9))/E \tag{70}$$

where $E = 252(1+\eta+\eta^2) + 672(\eta^3+\eta^4)$. Then, define

$$\alpha_0 = A(-108,-288)r_1^2 + B(96,180) + C(-320,-152)r_1^{-3} + D(384,114)r_1^{-5} \tag{71}$$

$$\alpha_1 = A(-30,-80)r_1^2 + B(48,90) + C(0,0)r_1^{-3} + D(32,19/2)r_1^{-5} \tag{72}$$

$$\alpha_2 = A(-36,-96)r_1^2 + B(96,180) + C(160,76)r_1^{-3} + D(-96,-57/2)r_1^{-5} \tag{73}$$

$$\alpha_3 = A(-48,-128)r_1^2 + B(48,90) + C(80,38)r_1^{-3} + D(-128,-38)r_1^{-5} \tag{74}$$

Note that $A(-108,-288) = -3/7$, $A(-30,-80) = -5/42$, $A(-36,-96) = -1/7$, and $A(-48,-128) = -4/21$. We find that the coefficient of r_1^{-3} in α_3 is a factor of 2 smaller than is given in Peale and Cassen (1978). Otherwise, these expressions reproduce the numbers given in the appendix of Peale and Cassen (1978).

Also, let

$$G(x) = F(19,64,64,24) + xF(-228,672,-672,228) \tag{75}$$

where $x = \mu/(\rho g R)$, for rigidity μ, density ρ, surface gravity g, and radius R, and where

$$F(a,b,c,d) = a(\eta^7+\eta^8+\eta^9) + b(\eta^5+\eta^6) + c(\eta^3+\eta^4) + d(1+\eta+\eta^2) \tag{76}$$

then define

$$k_2'(x) = E/G(x) \tag{77}$$

For $\mu = 6.5\times10^{11}$, $\rho = 3.34$, $g = 162$, and $R = 1.738\times10^8$ (all in cgs), we find $k_2' = 0.2649$, for $\eta = 1/2$, and $k_2' = 2.027$, for $\eta = 0.95$, which are in satisfactory agreement with the appendix in Peale and Cassen (1978).

Algebraically, the choice of E is arbitrary, since the strain depends on the product of k_2' and the α_i and this product is independent of E. Given the notation k_2' one might have expected it to reduce to the Love number k_2 for a homogeneous body when $\eta = 0$, but this is not the case. For $\eta = 0$, $k_2'(x) = (21/2)/(1+(19/2)x) = 7k_2$. So the reason for the choice of the factor E is a mystery; it looks like it should have had 1/7 the value it was given. Hence, we will choose $E' = E/7$. Define $A' = 7A$, $B' = 7B, C' = 7C$, and $D' = 7D$, then $\alpha_i' = 7\alpha_i$. And then we can set $k_2(x) = k_2'(x)/7$. This $k_2(x)$ has the expected value $(3/2)/(1+(19/2)x)$ for $\eta = 0$. And the coefficients in Eqs. (10)–(15) in Peale and Cassen (1978) can be recognized as α_i' for $\eta = 0$.

The strains are:

$$e_{rr} = \frac{k_2R}{g}\sum_{m,p,q}\alpha_0'(r_1)\left(\frac{V_{2mpq}}{r^2}\right) \tag{78}$$

$$e_{\theta\theta} = \frac{k_2R}{g}\sum_{m,p,q}\left[\alpha_1'(r_1)\frac{\partial^2}{\partial\theta^2}\left(\frac{V_{2mpq}}{r^2}\right) + \alpha_2'(r_1)\left(\frac{V_{2mpq}}{r^2}\right)\right] \tag{79}$$

$$e_{\phi\phi} = \frac{k_2R}{g}\sum_{m,p,q}\left[\alpha_1'(r_1)\left(\frac{-m^2}{\sin^2\theta} + \cot\theta\frac{\partial}{\partial\theta}\right)\left(\frac{V_{2mpq}}{r^2}\right) + \alpha_2'(r_1)\left(\frac{V_{2mpq}}{r^2}\right)\right] \tag{80}$$

$$e_{r\theta} = \frac{k_2R}{g}\sum_{m,p,q}\alpha_3'(r_1)\frac{\partial}{\partial\theta}\left(\frac{V_{2mpq}}{r^2}\right) \tag{81}$$

$$e_{r\phi} = \frac{k_2R}{g}\sum_{m,p,q}\alpha_3'(r_1)\frac{1}{\sin\theta}\frac{\partial}{\partial\phi}\left(\frac{V_{2mpq}}{r^2}\right) \tag{82}$$

$$e_{\theta\phi} = \frac{k_2R}{g}\sum_{m,p,q}\left[\frac{\alpha_1'(r_1)}{\sin\theta}\left(\frac{\partial^2}{\partial\theta\partial\phi} - \cot\theta\frac{\partial}{\partial\phi}\right)\left(\frac{V_{2mpq}}{r^2}\right)\right] \tag{83}$$

This corrects a typo in Eq. (82) in Peale and Cassen (1978).

Given the strains, we can compute the local rate of energy dissipation per unit mass and, by integration, the total rate of energy dissipation. The local rate of energy dissipation is, from Peale and Cassen (1978), Eq. (17),

$$H = \sum_{ij} 2\mu e_{ij}\dot{e}_{ij}^* \tag{84}$$

where the dot indicates time derivative and the $*$ indicates that the phase of each term is given a phase lag of $1/Q_{2mpq}$. Keeping only the potential terms $(lmpq) = (2,0,1,1)$, (2,0,1,−1), (2,2,0,1), and (2,2,0,−1), which are the most important terms for synchronous rotation in an eccentric non-inclined orbit, we find that the integral of the local dissipation over angles gives

$$\frac{dE_r}{dt} = \frac{2\pi2\mu G^2M^2e^2k_2^2R^2n}{a^6Qg^2}\left(-126(\alpha_1')^2 + \frac{252}{5}\alpha_1'\alpha_2' - \frac{42}{5}(\alpha_2')^2 - \frac{21}{5}(\alpha_0')^2 - \frac{252}{5}(\alpha_3')^2\right) \tag{85}$$

In this case all the phase lags have the same frequency, so we assume they have the same magnitude.

For $\eta = 0$ this becomes

$$\left.\frac{dE_r}{dt}\right|_{\eta=0} = \frac{2\pi2\mu G^2M^2e^2k_2^2R^2n}{a^6Qg^2}\left(224 + -392r_1^2 + \frac{1813}{10}r_1^4\right) \tag{86}$$

where $r_1 = r/R$. Multiplying by r^2 and integrating from 0 to R, gives the total rate of energy dissipation

$$\left.\frac{dE}{dt}\right|_{\eta=0} = \frac{2\pi2\mu G^2M^2e^2k_2^2R^5n}{a^6Qg^2}\frac{133}{6} \tag{87}$$

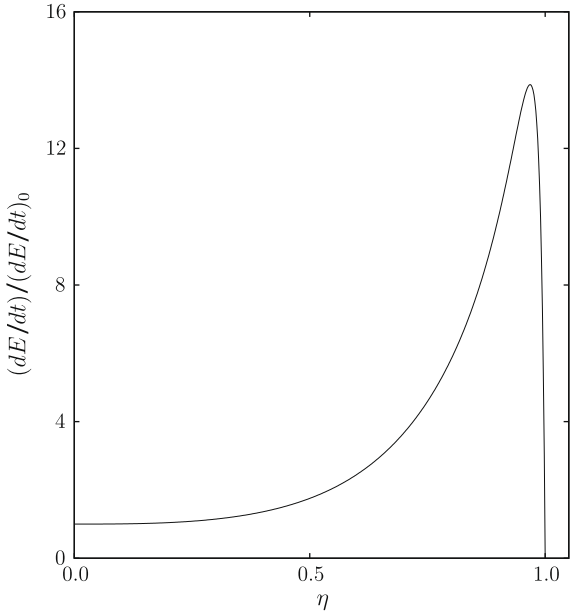

Fig. 6. Recalculation of Fig. 1 from Peale et al. (1979). This shows the ratio of the total dissipation in the two-layer model to the total dissipation in a homogeneous body ($\eta = 0$) plotted versus η, the fractional thickness of the interior.

Using $g = Gm/R^2$, where $m = (4/3)\pi\rho R^3$, and replacing one factor of k_2 by $(3/2)/(1 + (19/2)x)$, which for large $x = \mu/(2\rho g R)$ becomes

$$k_2 \approx \frac{3\rho g R}{19\mu} \tag{88}$$

we obtain

$$\left.\frac{dE}{dt}\right|_{\eta=0} = \frac{21}{2}\frac{GM^2e^2R^5n}{a^6}\frac{k_2}{Q} \tag{89}$$

This is the usual expression for tidal heating (Peale and Cassen, 1978, see also Peale, 2003; Wisdom, 2008). Note that we had to make a large μ approximation to get it.

More generally, the angle integrated rate of tidal dissipation is given by Eq. (85). The radial integral can be done analytically, but the expression is complicated, so will not be displayed. Fig. 6 shows the total tidal heating in the two-layer model as a function of η, for Io parameters ($R = 1.821 \times 10^8$, $\rho = 3.53$, $g = 179.71$, $\mu = 6.5 \times 10^{11}$, in cgs). This recalculates Fig. 6 from Peale et al. (1979). The agreement is not perfect, but they do not give the assumed values of their parameters, and there was a factor of 2 error (typographical error?) in one of their coefficients.

References

Abe, Y., 1993. Physical state of the very early Earth. Lithos 30, 223–235.

Abe, Y., 1997. Thermal and chemical evolution of the terrestrial magma ocean. Phys. Earth Planet. Interiors 100, 27–39.

Cherniak, D.J., Watson, E.B., 2003. Diffusion in zircon. In: Hanchar, J.M., Hoskin, P.W.O. (Eds.), Zircon, Reviews in Mineralogy and Geochemistry, vol. 53, pp. 113–139.

Connelly, J., Amelin, Y., Krot, A., Bizzarro, M., 2008. Chronology of the Solar System's oldest solids. Astrophys. J. 675, 121–124.

Deer, W.A., Howie, R.A., Zussman, J., 1996. An Introduction to the Rock-forming Minerals. Prentise-Hall, New York, 323 pp.

Efroimsky, M., Williams, J.G., 2009. Tidal Torques: A Critical Review of Some Techniques. CMDA 104, 257–289.

Elkins-Tanton, L.T., 2008. Linked magma ocean solidification and atmospheric growth for Earth and Mars. Earth Planet. Sci. Lett. 271, 181–191.

Garrick-Bethell, I., Wisdom, J., Zuber, M., 2006. Evidence for a past high eccentricity lunar orbit. Science 313, 652–655.

Garrick-Bethell, I., Weiss, B.P., Shuster, D.L., Buz, J., 2009. Early lunar magnetism. Science 323, 356–359.

Ghiorso, M.S., Sack, R.O., 1995. Chemical mass transfer in magmatic processes. IV. A revised and internally consistent thermodynamic model for the interpolation and extrapolation of liquid–solid equilibria in magmatic systems at elevated temperatures and pressures. Contrib. Mineral. Petrol. 119, 197–212.

Goldreich, P., 1966. History of the lunar orbit. Rev. Geophys. 4, 411–439.

Goldreich, P.M., Mitchell, J.L., 2009. Elastic ice shells of synchronous moons: Implications for cracks on Europa and non-synchronous rotation of Titan. Icarus, submitted for publication. arXiv:0910.0032.

Hut, P., 1981. Tidal evolution in close binary systems. Astron. Astrophys. 99, 126–140.

Kokubo, E., Canup, R.M., Ida, S., 2000. Lunar accretion from an impact-generated disk. In: Canup, R.M., Righter, K. (Eds.), Origin and of the Earth and Moon. University of Arizona, pp. 145–163.

Levrard, B., Correia, A.C.M., Chabrier, G., Baraffe, I., Selsis, F., Laskar, J., 2007. Tidal dissipation within hot Jupiters: A new appraisal. Astron. Astrophys. 462, L5–L8.

Longhi, J., 2003. A new view of lunar ferroan anorthosites: Postmagma ocean petrogenesis. J. Geophys. Res. 108, 1–16.

Matsuyama, I., Nimmo, F., 2008. Tectonic patterns on reoriented and despun planetary bodies. Icarus 195, 459–473.

Mignard, F., 1979. The evolution of the lunar orbit revisited, I. Moon Planets 20, 301–315.

Mignard, F., 1980. The evolution of the lunar orbit revisited, II. Moon Planets 23, 185–201.

Mignard, F., 1981. The lunar orbit revisited, III. Moon Planets 24, 189–207.

Nemchin, A., Timms, N., Pidgeon, R., Geisler, T., Reddy, S., Meyer, C., 2009. Timing and crystallization of the lunar magma ocean constrained by the oldest zircon. Nat. Geosci. 2, 133–136.

Ojakangas, G.W., Stevenson, D.J., 1986. Episodic volcanism of tidally heated satellites with application to Io. Icarus 66, 341–358.

Peale, S.J., 2003. Tidally induced volcanism. CMDA 87, 129–155.

Peale, S.J., Gold, T., 1965. Rotation of the planet Mercury. Nature 206, 1240–1241.

Peale, S.J., Cassen, P., 1978. Contribution of tidal dissipation to lunar thermal history. Icarus 36, 245–269.

Peale, S.J., Cassen, P., Reynolds, R., 1979. Melting of Io by tidal dissipation. Science 203, 892–894.

Plummer, H.C., 1960. An Introductory Treatise on Dynamical Astronomy. Dover, New York, 44 pp.

Ray, R.D., Eanes, R.J., Lemoine, F.G., 2001. Constraints on energy dissipation in the Earth's body tide from satellite tracking and altimetry. Geophys. J. Int. 144, 471–480.

Smith, J.V., Anderson, A.T., Newton, R.C., Olsen, E.J., Wyllie, P.J., Crewe, A.V., Isaacson, M.S., Johnson, D., 1970. Petrologic history of the Moon inferred from petrography, mineralogy, and petrogenesis of Apollo 11 rocks. Proc. Apollo 11 Lunar Planet. Sci. Conf. 897–925.

Snyder, G.A., Taylor, L.A., Neal, C.R., 1992. A chemical model for generating the sources of mare basalts: Combined equilibrium and fractional crystallization of the lunar magmasphere. Geochim. Cosmochim. Acta 56, 3809–3823.

Solomon, S., 1986. On the early thermal state of the Moon. In: Hartmann, W.K., Philips, R.J., Taylor, G.J. (Eds.), Origin of the Moon. LPI, Houston, pp. 435–452.

Thompson, C., Stevenson, D., 1988. Gravitational instability in two-phase disks and the origin and the Moon. Astrophys. J. 333, 452–481.

Touboul, M., Kleine, T., Bourdon, B., Palme, H., Wieler, R., 2007. Late formation and prolonged differentiation of the Moon inferred from W isotopes in lunar metals. Nature 450, 1206–1209.

Touma, J., Wisdom, J., 1994. Evolution of the Earth–Moon System. Astron. J. 108, 1943–1961.

Touma, J., Wisdom, J., 1998. Resonances in the early evolution of the Earth–Moon system. Astron. J. 115, 1653–1663.

Turcotte, D.L., Schubert, G., 2002. Geodynamics. Cambridge University Press, Cambridge, 137 pp.

Vening Meinesz, F.A., 1947. Shear patterns of the Earth's crust trans. Am. Geophys. Union 28, 1–61.

Ward, W.R., 1975. Past orientation of the lunar spin axis. Science 189, 377–379.

Warren, P.H., 1986. The bulk-Moon MgO/FeO ratio: A highlands perspective. In: Hartmann, W.K. (Ed.), Origin of the Moon. Lunar and Planetary Institute, pp. 279–310.

Wieczorek, M.A., Phillips, R.J., 1999. Lunar multiring basins and the cratering process. Icarus 139, 246–259.

Williams, J.G., Boggs, D.H., Yoder, C.F., Ratcliff, J.T., Dickey, J.O., 2001. Lunar rotational dissipation in solid body and molten core. J. Geophys. Res. 106, 27933–27968.

Wisdom, J., 2006. Dynamics of the lunar spin axis. Astron. J. 131, 1864–1871.

Wisdom, J., 2008. Tidal dissipation at arbitrary eccentricity and obliquity. Icarus 193, 637–640.

Wood, J.A., Dickey, J.S., Marvin, U.B., Powell, B.N., 1970. Lunar anorthosites and a geophysical model of the Moon. Proc. Apollo 11 Lunar Planet. Sci. Conf. 965–988.

Yin, Q., Jacobsen, S.B., Yamashita, K., Blichert-Toft, J., Telouk, P., Albarède, F., 2002. A short timescale for terrestrial planet formation from Hf–W chronometry of meteorites. Nature 418, 949–952.